Mesoporous Bioactive Glass Nanoparticles Promote Odontogenesis and Neutralize Pathophysiological Acidic pH

Wenyan Huang[1†], Jingjing Yang[1†], Qiong Feng[1], Yan Shu[1,2], Cong Liu[3], Shihan Zeng[3], Hongbing Guan[1], Lihong Ge[1,4]*, Janak L. Pathak[1]* and Sujuan Zeng[1]*

[1] Guangzhou Key Laboratory of Basic and Applied Research in Oral Regenerative Medicine, Affiliated Stomatology Hospital of Guangzhou Medical University, Institute of Oral Disease, Guangzhou Medical University, Guangzhou, China, [2] Department of Pharmaceutical Sciences, School of Pharmacy, University of Maryland, Baltimore, MD, United States, [3] National Engineering Research Center for Tissue Restoration and Reconstruction, South China University of Technology, Guangzhou, China, [4] Department of Pediatric Dentistry, Peking University Hospital of Stomatology, Beijing, China

Pathophysiological acidic-pH hinders the dental biomaterial-based pulp-dentin regeneration. Bioactive glass (BG) synthesized by sol-gel methods had shown odontogenic and pulp regeneration potential. However, the pathophysiological acidic-pH neutralizing potential of BG has not been tested yet. In this study, we aimed to design mesoporous BG-nanoparticles by a well-established sol-gel method and test its odontogenic and acidic-pH neutralizing potential. BG-nanoparticles were synthesized and further characterized by SEM, EDS, XRD, and FTIR. Mono-dispersed and spherical mesoporous BG-nanoparticles with size 300–500 nm were successfully fabricated. Effect of BG ionic extraction in DMEM with 0.1–2.5 g/L BG concentrations on proliferation and odontogenic differentiation of stem cells from human exfoliated deciduous teeth (SHED) was analyzed. All the BG ionic extractions did not affect SHEDs proliferation at early time points (day 1 and 3). BG ionic extraction 0.5 g/L robustly enhanced odontogenic differentiation of SHEDs, as shown by the expression pattern of ALP, Col1, DSPP, and matrix mineralization results. The chemical composition of the BG ionic extraction-induced mineralized matrix resembled natural dentin. BG-nanoparticles/alginate paste neutralized the butyric acid solution (pH 5.4) and buffered within pH 8.3 for a month. Our findings showed the odontogenic and pathophysiological acidic-pH neutralizing potential of BG-nanoparticles, indicating its possible application in pulp-dentin regeneration under pathophysiologically challenged acidic environment.

Keywords: bioactive glass nanoparticles, odontogenic differentiation, pulp-dentin regeneration, acidic pH, odontogenesis

INTRODUCTION

Dentin and pulp tissue damage are mainly caused by bacterial activity, chemical erosion, and trauma. Dentin and pulp tissue damage are among the most common dental problems that substantially impact patient oral health and quality of life (Shah et al., 2020). After the introduction of restorative mineral trioxide aggregate (MTA) as a sealing agent in the early 1990s, pulpotomy

to protect the damaged tooth entered a new era (Lee et al., 1993). The conventional calcium hydroxide-based biomaterials are still the primary choice for dental caries repair and pulp capping (Parirokh et al., 2018). However, calcium hydroxide-based biomaterials, including MTA, have numbers of limitations, such as long solidification time, poor handling performance, toxicity, postoperative tooth discoloration, and high cost (Parirokh and Torabinejad, 2010; Parirokh et al., 2018). Therefore, novel cost-effective biomaterials for dentin and pulp tissue repair are still in high demand.

With recent advances in biomaterials design, researchers around the world are focused on developing novel dental biomaterials with dentin and pulp tissue restorative and regenerative properties. Bioactive glass (BG) is a highly biocompatible and osteoinductive silicate biomaterial (Rahaman et al., 2011). Ionic dissolution products from BG (e.g., Si, Ca, and P) are closely related to its biological and physiochemical activities (Hench and Polak, 2002; Hench and Jones, 2015). BG ionic dissolution products develop a hydroxycarbonate apatite (HCA) layer that promotes tissue regeneration. The HCA layer creates a strong bond between BG and hard tissues. BG-based biomaterials are biocompatible, angiogenic, immunomodulatory, antibacterial, and anti-inflammatory (Kargozar et al., 2018; Zeng et al., 2018; Zhou et al., 2018; Lin et al., 2019). Since BG is relatively low cost biomaterial, it possesses the potential to be the cost effective biomaterial for pulp-dental regeneration. BG is analogous to MTA, except the MTA has crystalline calcium phosphates structure, and BG has silicon-oxygen inorganic networks containing amorphous structure with robust biological activity. Dentin and pulp tissue regeneration are complex biological processes, involving odontogenesis, angiogenesis, immunomodulation, inflammation, and neuronal signaling (Shah et al., 2020). BG biomaterials had shown promising potential to regenerate various tissue, including bone, cartilage, skin, nerve, and periodontal tissue (Marquardt et al., 2014; Yu et al., 2016; Barbeck et al., 2017; Farano et al., 2019; Gomez-Cerezo et al., 2019). BG had been reported to enhance the odontogenic differentiation of precursor cells (Gong et al., 2014; Wang et al., 2014). Therefore, BG-based biomaterials hold potential for dentin/pulp tissue restoration/regeneration.

Mesoporous BG nanoparticles had been reported to enhance antimicrobial and tissue regenerative potential (Vichery and Nedelec, 2016). The sol-gel method is a widely accepted method of mesoporous BG nanoparticle fabrication for biomedical applications (Hu et al., 2018). Excessive bacterial localization-induced acidic pH in the decayed tooth is a key hurdle during the dentin and pulp tissue regeneration. The bacterial and inflammatory milieu with acidic pH in the decayed tooth affects the physicochemical properties of restorative/regenerative sealing materials (Elnaghy, 2014). Moreover, acidic pH impairs cell viability and tissue-specific differentiation of precursor cells. The sealing materials with the potential to neutralize the acidic pH in the affected tooth and pulp tissue have not been reported so far. Therefore, it is wise to design the bioactive restorative/regenerative dental materials that could neutralize the acidic pH and maintain the physicochemical properties of biomaterials and cellular activity.

In this study, we aimed to fabricate mesoporous BG nanoparticles by well-established sol-gel method and analyze its acidic pH neutralizing and odontogenic potential. The mesoporous BG nanoparticles were successfully synthesized and characterized. The release of Si, Ca, and P ions in neutral pH and acidic pH, as well as in regular cell culture medium, were analyzed. The effect of BG nanoparticles ionic extract on stem cells from human exfoliated deciduous teeth (SHEDs) proliferation, odontogenic differentiation, and dentin like matrix mineralization was analyzed. The acidic pH simulating the pathophysiological pH during dental erosion and pulp damage was neutralized by mesoporous BG nanoparticles/alginate paste for 30 days *in vitro*. The BG ionic extract robustly enhanced odontogenic differentiation of SHEDs and dentin-like matrix mineralization, indicating its application in pulp-dentin regeneration of decayed teeth with pathophysiologically challenged acidic pH.

MATERIALS AND METHODS

Preparation of Mesoporous BG Nanoparticles

Mesoporous BG nanoparticles were synthesized by the sol-gel method as described previously (Li et al., 2017; Hu et al., 2018), with a slight modification in the contents of SiO_2, CaO, and P_2O_5 (wt %) used. Briefly, the procedure was designed to use the molar composition of 58% SiO_2 (mass fraction), 33% CaO, and 9% P_2O_5. Dodecylamine (DDA, Aladdin) was used as a catalyst and template. DDA (4 g) was dissolved in 25 mL of deionized water (DW) and 80 mL of absolute ethanol (EtOH, Guanghua Chemical). Then, 16 mL of tetraethyl orthosilicate (TEOS, Guanghua Chemical) was added to the DDA solution and stirred for 1 h. 1.21 ml triethyl phosphate (TEP, Aladdin) and 3.32 g calcium nitrate tetrahydrate (CN, Guanghua Chemical) were added subsequently in 30 min interval under magnetic stirring at 40°C. The resulting solution was vigorously stirred for another 3 h. The white precipitate was collected by three times filtration and rinsing with absolute ethanol and deionized water. The filtrate was freeze-dried for 24 h. The BG nanoparticles were obtained by removing the templates and organic components by sintering at 650°C for 3 h (2°C/min).

Physicochemical Characterization of BG Nanoparticles

The morphology and elemental composition of BG nanoparticles were characterized by scanning electron microscope equipped with an energy-dispersive X-ray spectrometer (SEM-EDX, Hitachi S-3400N II, Model 550i, Japan). The phase composition analysis was assessed by X-ray diffraction (XRD, Bruker D8 AVANCE equipped with a LYNXEYE detector, Bruker AXS, Karlsruhe, Germany). Chemical structure analysis was performed by Fourier transform infrared spectroscopy (FTIR, Thermo Nicolet IS10, United States) with a wavenumber range from 500 to 4000 cm^{-1}.

BG Ionic Extraction Preparation for *in vitro* Cell Culture

The BG nanoparticles ionic extraction was prepared by incubating BG nanoparticles in DMEM (Gibco, United States) at the concentration of 10 g/L at 37°C and 120 rpm/min for 24 h, as described previously (Gong et al., 2014). BG-DMEM solution 10 g/L was further diluted to 0.1, 0.5, and 2.5 g/L. Particulates were removed by filtration through a 0.22 μm filter (Millipore, United States). The elementary content of silicon (Si), calcium (Ca), and phosphorus (P) ions in BG ionic extraction was determined by ICP-OES analysis (Agilent, United States). All BG ionic extraction in DMEM with 0.1, 0.5, and 2.5 g/L of BG were supplemented with 10% fetal bovine serum (Gibco, United States), 100 mg/mL streptomycin, and 100 U/mL penicillin and used for cell culture.

Isolation and Characterization of SHEDs

The deciduous teeth (6 incisors) were all collected from the 6–8 years old patients visiting the Pediatric Dentistry Department of Affiliated Stomatology Hospital of Guangzhou Medical University. The written informed consents were obtained from the patients' parent. The Research Ethics Committee of Guangzhou Medical University approved this study (KY2019008). The inclusion criteria for the primary tooth were: lower deciduous tooth, root resorption less than 1/3, no dental cavities, and no periapical disease. There was no history of systemic and hereditary diseases in these patients.

The deciduous tooth and the peripheral area were thoroughly disinfected with 1% tincture iodine before extraction. After extraction, the tooth was washed with saline for 2 times, put in 4°C DEME medium containing 5 times penicillin/streptomycin for up to 4 h before SHEDs isolation. SHEDs were isolated, as described previously (Miura et al., 2003). The SHEDs of the third passage were labeled with fluorescein isothiocyanate-conjugated or phycoerythrin-conjugated antibodies and analyzed with flow cytometry. Cell aliquots (2.0×10^6 cells) were incubated for 0.5 h at 4°C with monoclonal antibodies specific for human CD45, CD34, CD19, CD105, CD90, and CD73 (BD Biosciences), or isotype-matched control IgGs (Southern Biotechnology Associates). After the cells were washed with stain buffer for 2 times, the cells were incubated with a secondary antibody at 4°C for another 30 min. The expression profiles for the cell surface markers were analyzed by flow cytometry (Calibur, BD Biosciences).

Cell Proliferation Assay

SHEDs (passage 5) were seeded at a density of 2.0×10^3 cells/well into 96-well plates with routine DEME contained with 10% fetal bovine serum, 100 mg/mL streptomycin, and 100 U/mL penicillin. After 24 h, the culture medium was replaced with fresh medium containing the above-mentioned BG ionic extractions (0, 0.1, 0.5, and 2.5 g/L). The fresh BG ionic extraction medium was changed every 2 days. At days 1, 3, 5, and 7, cell proliferation was analyzed by using the CCK8 assay (Dojindo, Japan) as described previously (Wang et al., 2020).

Alkaline Phosphatase (ALP) Activity and ALP Staining

Alkaline phosphatase (ALP) is a marker of odontogenic differentiation of precursor cells. SHEDs (passage 5) were seeded at a density of 2.0×10^4 cells/well into 48-well plates with routine DMEM. After 24 h, the culture medium was replaced with fresh BG ionic extraction medium. The fresh BG ionic extraction medium was changed in every 2 days. At 4 and 7 days, the ALP and total protein content in SHEDs' cultures were detected using an alkaline phosphatase assay kit and BCA quantitative detection kit (JianCheng Co., Nanjing, China), respectively, as described previously (Wang et al., 2020). The quantitative value of ALP activity was normalized with the total protein content. For ALP staining, at days 4 and 7, culture plates of SHEDs were fixed with a 4% paraformaldehyde solution and then stained with AKP kit (Beyotime, Shanghai, China).

Odontogenic Gene Expression Analysis

The expression of odontogenic markers, including ALP, collagen type I (COLI), and dentin sialophosphoprotein (DSPP), were detected by qRT-PCR. SHEDs (passage 5) were seeded at a density of 2.0×10^5 cells/well into 6-well plates with routine DMEM. After 24 h, the culture medium was replaced with fresh BG ionic extraction medium. The fresh BG ionic extraction medium was changed every 2 days. At 3, 7, and 10 days, the total RNA was extracted using a Trizol reagent (Invitrogen, Carlsbad, CA) according to the manufacturer's instructions. Two μg total RNA was reverse transcribed using cDNA kit (Invitrogen, Carlsbad, CA). Real-time (RT)-qPCR was performed using the SYBR Green qPCR kit (Qiagen, Germany) in iCycler IQMulti-color, Real time PCR Detection System. GADPH was used as a housekeeping gene. The following gene-specific primer sequences were used: ALP forward primer, 5′-GGACCATTCCCACGTCTTCAC-3′, and reverse primer, 5′-CCTTGTAGCCAGGCCCATTG-3′; COLI forward primer, 5′- CAGTGGTAGGTGATGTTCTGGGAG-3′, and reverse primer, 5′-CAAGAGGCATGTCTGGTTCGG-3′; DSPP forward primer, 5′-ATATTGAGGGCTGGAATGGGGA-3′, and reverse primer, 5′-TTTGTGGCTCCAGCATTGTCA-3′; GAPDH, 5′-GGACCTGACCTGCCGTCT AG-3', and reverse primer, 5'-GTAGCC CAGGATGCCCTTGA-3'.

Western Blot Analysis

After 1 and 3 days, the cultures were rinsed with PBS for 2 times. The cells were trypsinized and lysed. Proteins were quantitated with the bicinchoninic acid assay (BestBio, China). Total of 30 μg protein was separated by 10% sodium dodecyl sulfate-polyacrylamide gel electrophoresis and transferred to polyvinylidene fluoride (PVDF) membrane. The PVDF membrane was blocked with 5% skim milk at room temperature for 1 h and incubated with rabbit monoclonal anti-GAPDH (Abcam, United Kingdom) or human anti-DSPP (Bioss, China) primary antibody (1:1000 dilution) overnight at 4°C. Then PVDF membranes were incubated with HRP-conjugated goat anti-rabbit IgG (Abcam, United Kingdom)

secondary antibody (1:3000 dilution) 1 h at room temperature. The immunoblots were detected using a chemiluminescence kit (Millipore, United States) and photographed. ImageJ.1x (NIH. MD, United States) software was used to quantify band intensity.

In vitro Matrix Mineralization Assay

SHEDs (passage 5) were seeded at a density of 2.0×10^4 cells/well into 48-well plates with routine DEME. After 24 h, the culture medium was replaced with fresh BG ionic extraction medium. When the cells become 80% confluence, the cultures were supplemented with 50 µg/ml ascorbic acid, 5 mM β-Glycerophosphate, and 10 nM dexamethasone for odontogenic differentiation. For dentin mineralization assay, the cultures (day 14) were fixed with 70% ethanol and stained with 2% alizarin red (Sigma-Aldrich). Odontogenesis was determined by cellular accumulation of alizarin red-stained mineralized matrix. The mineralized matrix in different culture conditions was quantified as described previously (Yu et al., 2019).

Raman Spectroscopy for Native Dentin and in vitro Mineralized Matrix

After pulp tissue extraction, the deciduous tooth was stored in 1% chloramine T solution (Solarbio, China) at 4°C and polished with #320, 800, 1200, and 3000 mesh sandpaper in running water to expose the dentin. The deciduous tooth dentin and mineralized matrix in 0.5 g/L BG extraction treated culture were analyzed by a Raman Spectroscopy (LabRAM HR Evolution, HORIBA JY, France) operated with a diode laser of 785 nm wavelengths, a 2 cm^{-1} resolution and nominal laser power of 50 mW, for 20 s and 5 co-additions. The range of analysis was 200–2000 cm^{-1}. The data collection was controlled by the WINWIEW software. The fluorescence from the 48 average spectra was removed with a polynomial fitting of varying degrees using the OriginPro 2018 (OriginLab Corporation, MA, United States). Overall mean and standard deviation (SD) for peaks at 960, 1070, 1660 cm^{-1}, and ratios of 1070/960, 960/1660 were calculated based on 5 evaluations from each test layer of the 3 specimens (He et al., 2017). The peaks heights and ratios among the different dentin layers were compared. Mean mineral-to-matrix ratio values were calculated for native dental tissues and mineralized matrix in the BG ionic extraction treated SHEDs. Mineral-to-matrix ratio was calculated by dividing the area under the ∼960-cm^{-1} peak by the area under the Amide I peak at ∼1,660 cm^{-1} (Schwartz et al., 2012). The carbonate-to-phosphate ratio indicated carbonate substitution for phosphate and was calculated by dividing the area under the ∼1070-cm^{-1} peak by the area under the ∼960 cm^{-1} peak.

Acidic pH Neutralizing Capacity of Mesoporous BG Nanoparticles Paste

The BG nanoparticles were mixed with a phosphate buffer solution containing 1 wt% sodium alginate on a glass plate. The nanoparticles-to-solution ratio was ∼1.5 g/mL (Wang et al., 2014). The paste mixture was obtained by stirring and then filled to a sterile PTFE plastic ring (diameter 10 mm, height 3 mm). All the plastic rings were incubated at 37°C temperature and 5% CO_2 concentration for 12 h. Then BG/alginate paste was immersed in 10 mL aseptic PBS (pH = 7.4) or butyric acid (0.025% in PBS, pH = 5.4) and incubated on shaker at 37°C temperature and constant speed of 120 rpm/min for 5, 30 min, 1, 2, 4, 8, and 12 h, and 1, 2, 3, 4, 5, 6, 7, 14, 21, and 30 days. At each time point, the pH was determined using a twin pH meter (Mattler Toledo, Switzerland). On day 5, BG extractions were collected and filtered through a 0.45-mm microfiltration membrane. The elementary content of Si, Ca, and P ion in the solution was determined by ICP-OES analysis (Agilent, United States).

Statistical Analysis

All statistical calculations were performed with SPSSv.20.0 (SPSS Inc., Chicago, IL, United States) software. All data are expressed as mean ± standard deviation (SD). Differences between groups were analyzed using analysis of variance (ANOVA) followed by Bonferroni test. P value of <0.05 was considered statistically significant.
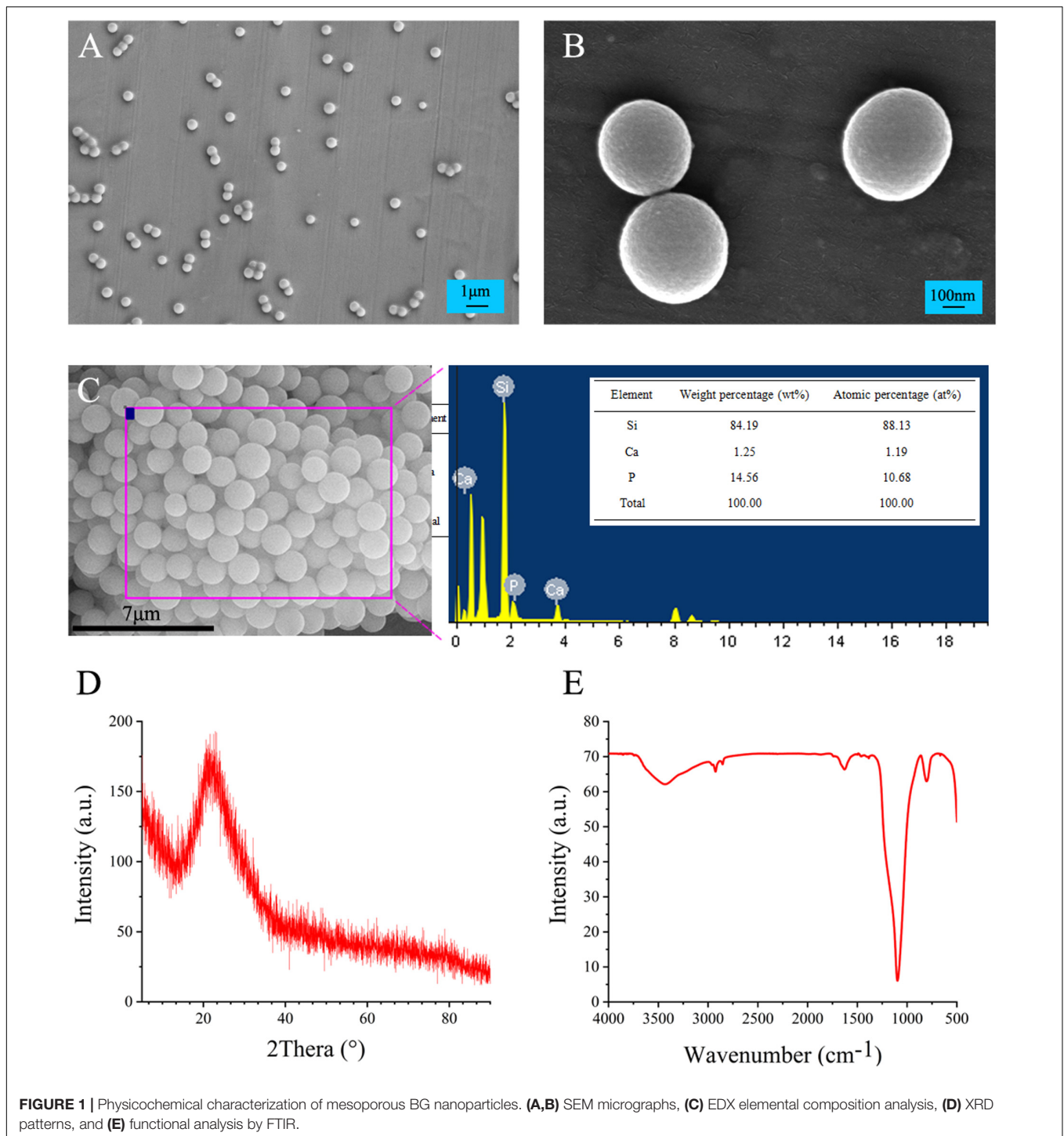
RESULTS

BG Nanoparticles Were Successfully Fabricated and Characterized

SEM images showed that mesoporous BG nanoparticles were formed with a regular spherical shape, mono dispersion, nanostructure, and size range 300–500 nm (**Figures 1A,B**). The EDX spectroscopy showed that BG nanoparticles are composed of silicon (84.19 wt%), calcium (14.56 wt%), and phosphorus (1.25 wt%) (**Figure 1C**).

The XRD results of BG nanoparticles showed the characteristic diffraction peaks of amorphous silicate materials in 15–30°, indicating the amorphous nature of BG nanoparticles (**Figure 1D**). The FTIR absorption spectrum of BG nanoparticles showed characteristic absorption peaks at 1090, 800, and 475 cm^{-1}, which in turn corresponds to typical Si-O-Si non-telescopic vibration peak, Si-O symmetrical expansion vibration peak, and Si-O-Si symmetrical bending vibration peak (**Figure 1E**).

Mesoporous BG Ionic Extraction in DMEM Showed the Dissolved Si, Ca, and P Ions

The concentration of Si in 0, 0.1, 0.5, and 2.5 g/L DMEM BG extractions-group was 1.84 ± 0.12, 15.46 ± 0.77, 54.64 ± 4.42, and 92.75 ± 2.49 mM, respectively (**Table 1**). The concentration of Si was very low in routine DMEM medium. The concentration of Si ion gradually increases in the groups with the increase of BG nanoparticles' concentration dissolved in DMEM. The ionic concentration of Ca in BG extractions was slightly higher than that in routine DMEM medium. The ionic concentrations of P in BG extractions were lower than that in routine DMEM medium,

FIGURE 1 | Physicochemical characterization of mesoporous BG nanoparticles. **(A,B)** SEM micrographs, **(C)** EDX elemental composition analysis, **(D)** XRD patterns, and **(E)** functional analysis by FTIR.

which may be related to the formation of hydroxyapatite carbonate on BG surface.

SHEDs Were Successfully Isolated From Deciduous Teeth and Characterized

The isolated SHEDs were photorefractive and adherent to the wall. After one week of culture, the cell population around the

tissue explants increased gradually, forming the appearance of cell colonies (**Figure 2A**). The cell morphology resembled to the fibroblasts (**Figure 2A**). The cells were polygonal or fusiform and adherent to the culture plate. The cells were stably cultured for up to 8 passages with consistent morphology and proliferation.

The FACs' results indicated that the MSCs' surface markers CD73, CD90, and CD105 were highly expressed in SHEDs, with an expression rate of ≥95% (**Figure 2B**). In

TABLE 1 | Si, Ca, and P ion concentration in BG ionic extraction in DMEM.

Group	Si (mg/L)	Ca (mg/L)	P (mg/L)
DMEM	1.84 ± 0.12	63.83 ± 0.47	30.4 ± 1.15
0.1 g/L BG-DMEM	15.46 ± 0.77	73.77 ± 1.20	25.45 ± 0.62
0.5 g/L BG-DMEM	54.64 ± 4.42	74.10 ± 1.28	25.13 ± 1.55
2.5 g/L BG-DMEM	92.75 ± 2.49	80.21 ± 1.49	22.44 ± 1.22

The data are presented as mean $\pm$ SD from 3 independent experiments (n = 3).

contrast, SHEDs did not show significant expression ($\leq 2\%$) of hematopoietic/endothelial origin stem cell markers, i.e., CD19, CD34, and CD45 (**Figure 3B**).

BG Ionic Extraction From Higher Concentration of BG Inhibited SHEDs Proliferation at Day 5 and 7

All the concentrations of BG ionic extraction treated (0.1, 0.5, and 2.5 g/L-group) did not affect SHEDs proliferation at days 1 and 3 (**Figure 3A**). BG ionic extraction (0.5 and 2.5 g/L-group) inhibited SHEDs proliferation at days 5 and 7 (**Figure 3A**). BG extractions 2.5 g/L-group showed higher inhibition on SHEDs proliferation at days 5 and 7 compared to BG extractions 0.5 g/L-group (**Figure 3A**).

BG Ionic Extraction 0.5 g/L-Group Induced the Highest Odontogenic Differentiation of SHEDs

BG ionic extraction 0.1 and 2.5 g/L-group did not affect, but 0.5 g/L-group enhanced ALP activity at day 4 by 1.4-fold compared to the control group (**Figure 3B**). Interestingly, BG ionic extraction 0.1, 0.5, and 2.5 g/L-group enhanced ALP activity at day 7 by 1. 7-, 2. 2-, and 1.9-fold, respectively, compared to the control group (**Figure 3B**). ALP protein expression at day 4 did not show noticeable differences between the control and BG ionic extraction treatment groups (**Figure 3C**). However, 0.1, 0.5, and 2.5 g/L-group showed higher ALP protein expression at day 7 compared to the control group, and 0.5 g/L-group showed the highest expression of ALP protein at day 7 compared to the other groups (**Figure 3C**). DSPP is another established marker of odontogenic differentiation. Protein level expression of DSPP was analyzed by western blot assay. All the BG ionic extraction groups tested in this study upregulated DSPP expression in SHEDs at day 1 and day 3 (**Figures 3D,E**).

We further analyzed the mRNA expression of odontogenic differentiation markers ALP, Col1, and DSPP in BG ionic extractions treated SHEDs at days 3, 7, and 10. The 0.1 g/L-group enhanced ALP expression at days 3 and 7, COL1 at day 7, and DSPP at day 3 (**Figure 4**). Interestingly, 0.5 g/L-group robustly upregulated the expression of ALP, COl1, and DSPP expression at days 3 and 7. However, 2.5 g/L-group did not affect ALP, COl1, and DSPP expression at days 3 and 7. All the treatment did not affect ALP, COl1, and DSPP expression at day 10 (**Figures 4A–C**).

BG Ionic Extraction 0.5 g/L-Group Induced the Highest Matrix Mineralization in SHEDs Culture

Alizarin red staining revealed that more matrix-mineralized nodules were generated in the BG extraction groups than in the control group after 2 weeks of culture (**Figure 5A**). BG extraction 0.5 g/L-group showed the most intense alizarin red staining compared to other groups (**Figure 5A**). Quantitative analysis of alizarin red staining showed that BG extraction 0.1 and 0.5 g/L-group showed 1.44- and 1.67-fold, higher matrix mineralization, compared to control group, respectively (**Figure 5B**).
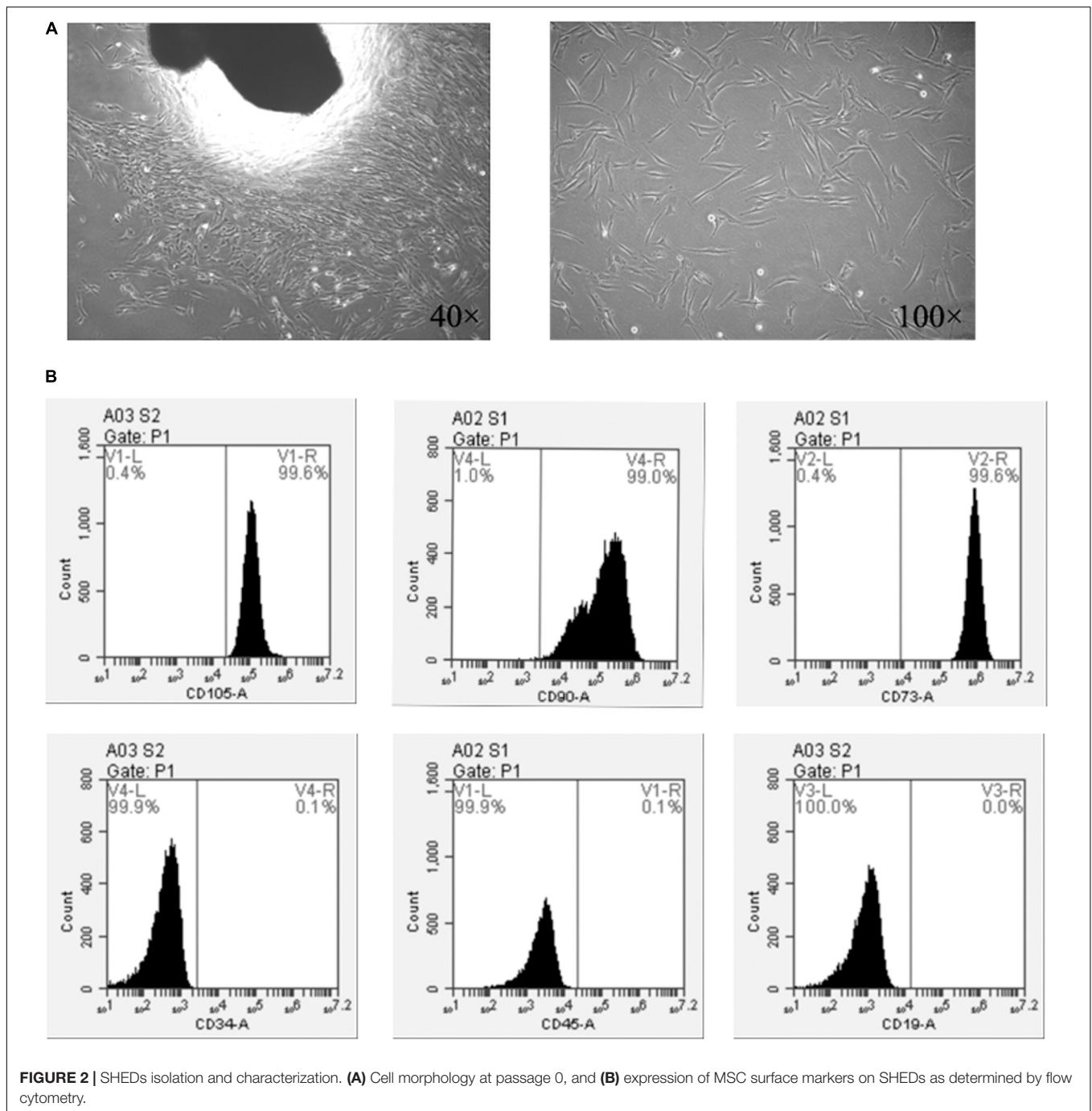
Mineral Contents in the Mineralized Matrix Resemble to Natural Dentin

As shown in **Figure 6**, the mineralized matrix showed a strong peak related to PO_4^{3-} vibration at 960 cm^{-1} band. As shown in **Figure 6** and **Table 2**, the mineralized matrix and natural dentin had similar spectral characteristics between 200–2000 cm^{-1} band and mineral/matrix ratio. Mineralized matrix showed slightly lower carbonate substitution and peak intensity of phosphate 960 cm^{-1} band, indicating that the calcium phosphate content of mineralized matrix *in vitro* was lower than that of the natural dentin. Besides, the characteristic peaks of organic components, including Amide III and Amide I, varied in the mineralized matrix.

The Ionic Release and Acidic pH Neutralization by BG Nanoparticles Paste

The Si and Ca ions concentrations in the solutions were increased while P ion concentration was decreased ($P < 0.05$), which may be related to the consumption of P in the process of hydroxyapatite formation. A low Si ion concentration was observed in butyric acid solution (pH 5.4) than in PBS (pH of 7.4) (**Figure 7**).
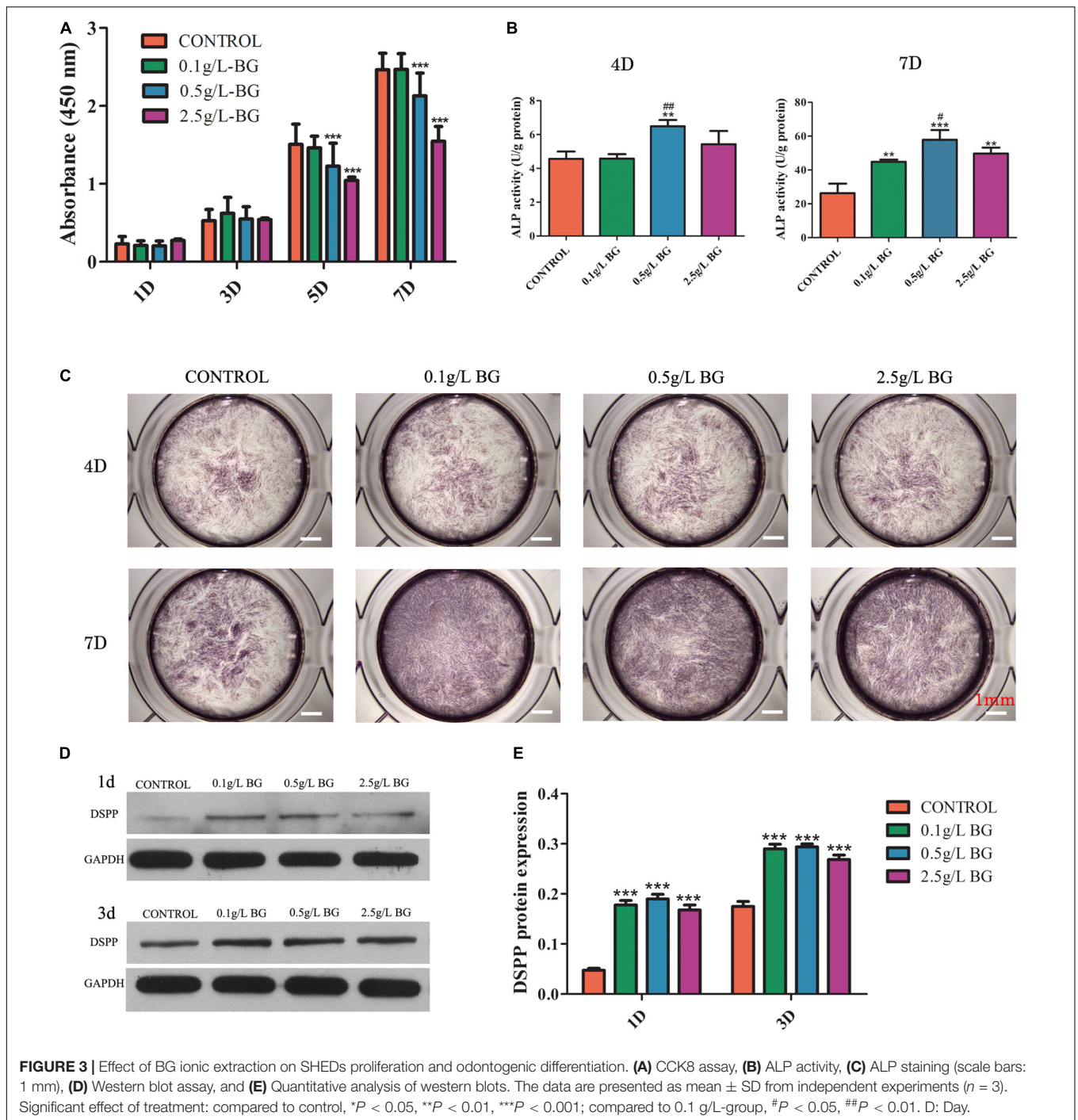
BG nanoparticles/alginate paste increased the pH value in both butyric acid solution (pH 5.4) and PBS (pH 7.4). In BG nanoparticles/alginate paste immersed PBS, the pH values increased slowly within the first 48 h, then tended to be stable (pH 9.32 ± 0.07). This result suggests the alkaline nature of BG ionic extraction. In BG nanoparticles/alginate paste immersed butyric acid solution, the pH value reached 7.13 at 24 h, then showed a slow continuous increase in pH and reached up to pH 8.34 on day 30. This result suggests that the BG ionic release could neutralize butyric acid solution (pH 7.4) and buffer it below pH 8.3 for a month. Under the acidic condition, the silicon hydroxyl groups are formed on the surface of BG and further create a silica gel membrane, which could hinder the ion exchange reaction and slows down the Si ion release. Such a porous gel membrane could allow the inner layer of BG to exchange slowly with the surrounding solution to form an alkaline environment (**Figure 8**).

FIGURE 2 | SHEDs isolation and characterization. **(A)** Cell morphology at passage 0, and **(B)** expression of MSC surface markers on SHEDs as determined by flow cytometry.
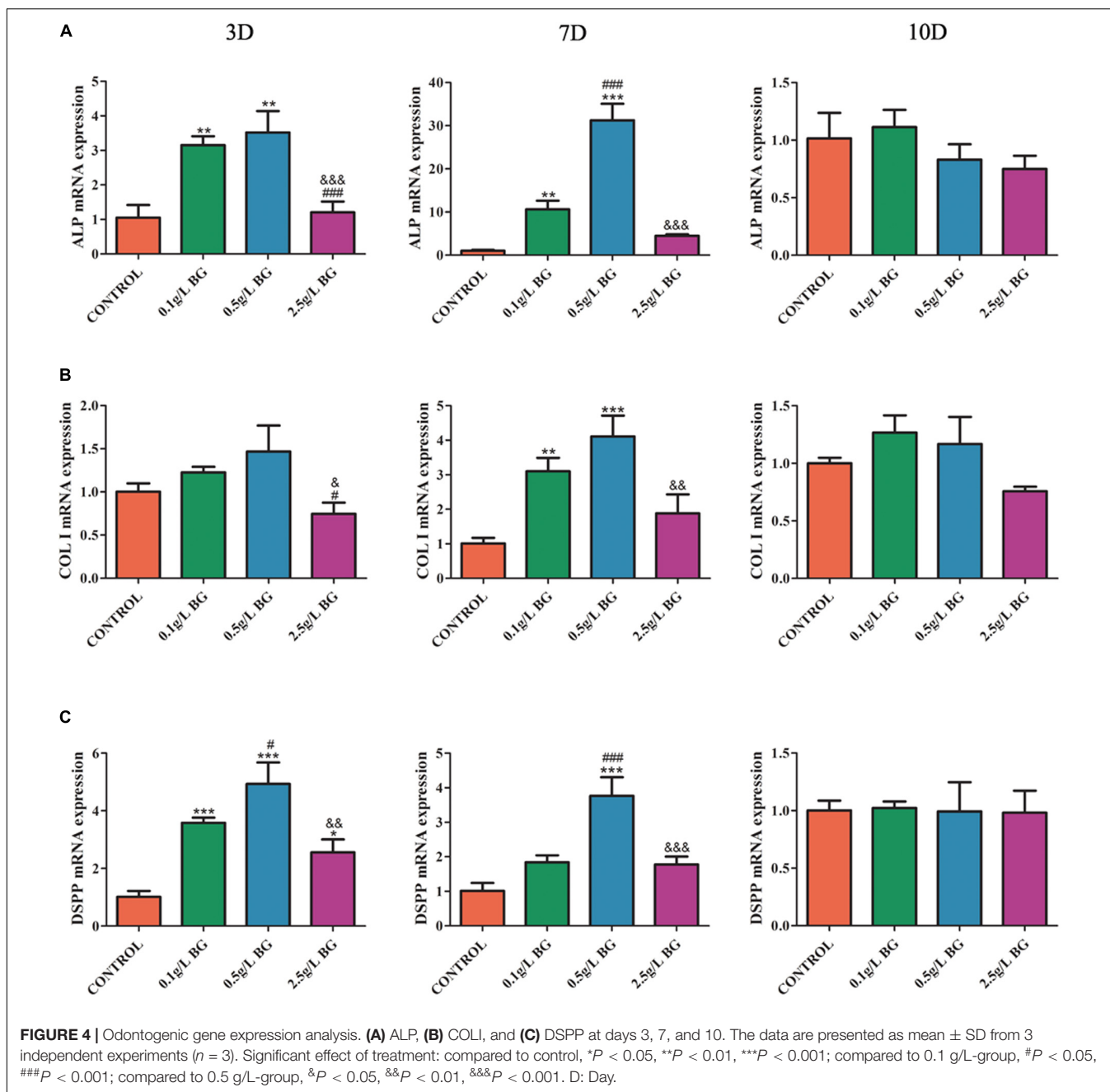
DISCUSSION

In clinical applications such as direct pulp capping and root canal lateral puncture repair, the pulp capping material directly contacts the tissue fluid and is exposed to local metabolic acidic environment caused by bacteria or inflammation. Anaerobic bacteria are dominant bacteria in pulp infection, and butyric acid, as one of the metabolic byproducts of anaerobic bacteria, is often used in the laboratory to simulate infectious acidic environments. Bacterial localization and pulpal/periapical inflammation-mediated acidic pH (pH ~5.5) hinders pulp-dentin regeneration (Loesche, 1996; Azuma, 2006; Hirose et al., 2016). Acidic pH in tooth lesions affects the physicochemical properties of the biomaterials and hinders the sealing potential, and inhibits cellular activity (Pushpa et al., 2018). Butyric acid is one of the bacterial byproducts causing acidic pH in and affecting dental/periodontal health and treatments (Niederman et al., 1997). Therefore, neutralizing the butyric acid-mediated acidic pH in dental and periodontal milieu could facilitate the treatment of dental/periodontal diseases. However, the dental

FIGURE 3 | Effect of BG ionic extraction on SHEDs proliferation and odontogenic differentiation. **(A)** CCK8 assay, **(B)** ALP activity, **(C)** ALP staining (scale bars: 1 mm), **(D)** Western blot assay, and **(E)** Quantitative analysis of western blots. The data are presented as mean ± SD from independent experiments ($n = 3$). Significant effect of treatment: compared to control, $*P < 0.05$, $**P < 0.01$, $***P < 0.001$; compared to 0.1 g/L-group, $^{\#}P < 0.05$, $^{\#\#}P < 0.01$. D: Day.
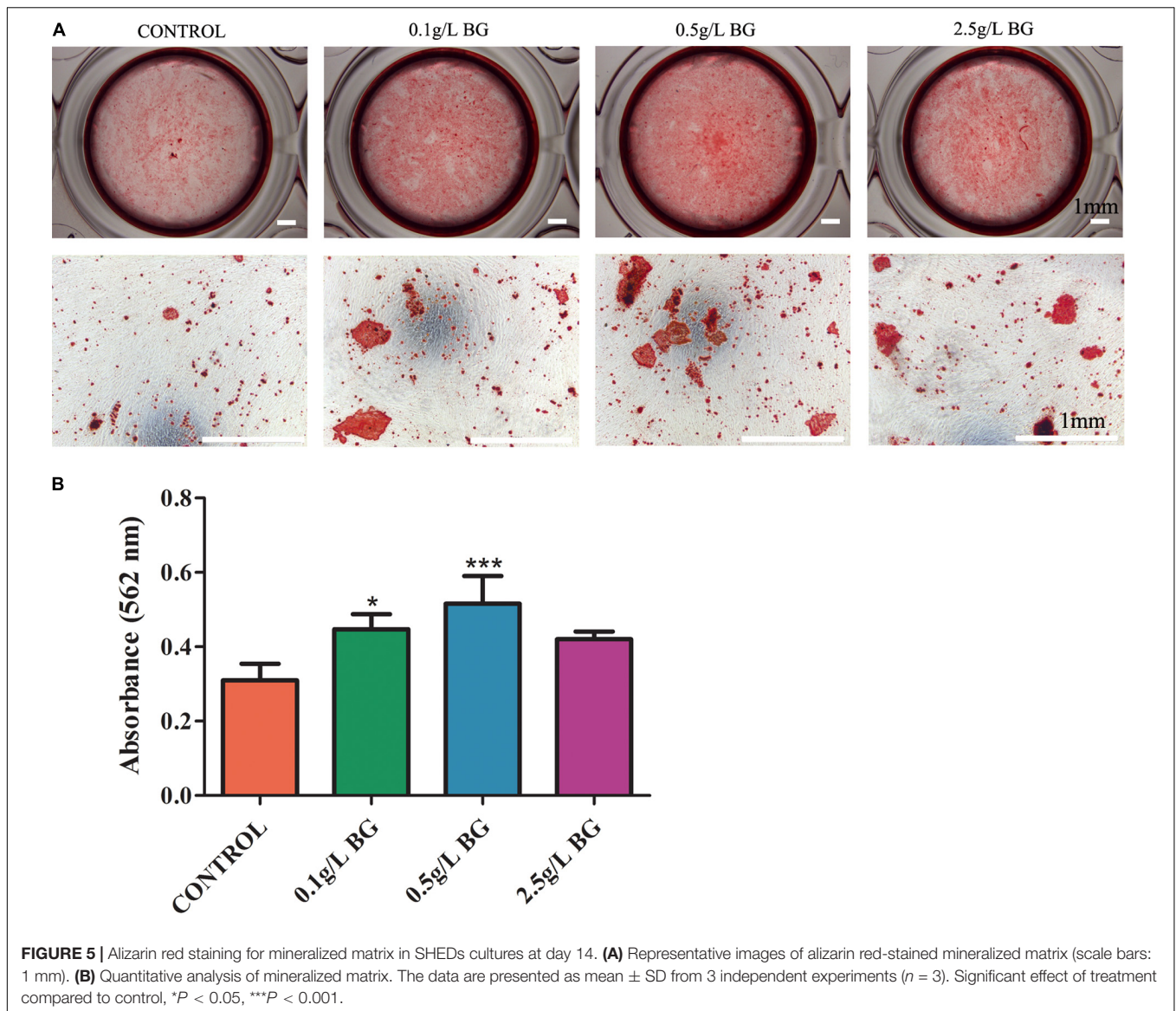
biomaterials that can neutralize the acidic pH and promotes pulp-dentin regeneration have not been reported yet. In this study, we fabricated the mesoporous BG nanoparticles with dentin regeneration and acidic pH neutralization potential. Butyric acid is the main metabolic byproduct of the anaerobic bacteria, which are predominantly localized in tooth lesions and infected dental pulp (Loesche, 1996). BG nanoparticles/alginate paste increases the pH 5.4 of butyric acid solution to pH 7.12 within 24 hrs. BG nanoparticles ionic extraction robustly

enhanced odontogenic differentiation of SHEDs and dentin like matrix mineralization in SHEDs culture. Our finding suggests the possible application of mesoporous BG nanoparticles in pulp-dentin regeneration under acidic pathophysiological environment. BG has shown robust potential for hard and soft tissue regeneration, including bone and skin (Hench and Polak, 2002; Hench and Jones, 2015). In recent years, scientific community is focused on developing various BG-based materials for various tissue regeneration applications. In

FIGURE 4 | Odontogenic gene expression analysis. **(A)** ALP, **(B)** COLI, and **(C)** DSPP at days 3, 7, and 10. The data are presented as mean ± SD from 3 independent experiments ($n = 3$). Significant effect of treatment: compared to control, $*P < 0.05$, $**P < 0.01$, $***P < 0.001$; compared to 0.1 g/L-group, $\#P < 0.05$, $\#\#\#P < 0.001$; compared to 0.5 g/L-group, $^\&P < 0.05$, $^{\&\&}P < 0.01$, $^{\&\&\&}P < 0.001$. D: Day.

dentistry, BG has been applied to treat periodontal disease, maxillofacial bone defect, dentin hypersensitivity, and dental defects in the form of a composite substrate material (Schepers et al., 1991; Lovelace et al., 1998; Skallevold et al., 2019). Most commonly used BG-based materials in dental clinics are prepared by the traditional melting method (Skallevold et al., 2019). The sol-gel-derived BG had shown superior bioactivity compared to the melting-derived BG (Li et al., 1991; Lei et al., 2012). This effect is mainly achieved by micro/mesoporous structure, uniform micron/submicron particle size, and large specific surface area. Moreover, sol-gel-derived BG quickly forms HCA increasing the bonding with bone or dentin (Hu

et al., 2018). The sol-gel method allows us to fabricate BG with micro to nanoscale size (Hu et al., 2018). Nanoscale biomaterials have shown a robust effect on cellular activity and tissue regenerative potential compared to macro/micro-scale biomaterials (Lei et al., 2012; Zhu et al., 2020). Mesoporous BG nanoparticles provide a large surface area and porosity that not only increases its bioactivity but also provides drugs carrier platform. In this study, we fabricated mono-dispersed mesoporous BG nanoparticles by slight modification in the previously described sol-gel method for BG preparation (Hu et al., 2018). The spherical and mono-dispersed mesoporous BG nanoparticles (300–500 nm diameter) were successfully

FIGURE 5 | Alizarin red staining for mineralized matrix in SHEDs cultures at day 14. **(A)** Representative images of alizarin red-stained mineralized matrix (scale bars: 1 mm). **(B)** Quantitative analysis of mineralized matrix. The data are presented as mean ± SD from 3 independent experiments (n = 3). Significant effect of treatment compared to control, $*P < 0.05$, $***P < 0.001$.

synthesized and characterized. Hu et al. (2014) previously reported the synthesis of bioactive mesoporous BG nanoparticles with a size range of 256–716 nm diameter using the sol-gel technique.

Among the various dental stem cells, SHEDs have a higher degree of stemness and are conveniently available from the pediatric dental clinic (Akpinar et al., 2014). Therefore, this study used SHEDs as a stem cell model for dentin regeneration. We successfully isolated and characterized SHEDs using established protocol (Miura et al., 2003). Biocompatibility of the biomaterials is vital for dentin and pulp regeneration therapy. We found that BG ionic extraction from 0.1–2.5 g/L BG did not affect the SHEDs viability at early time points (days 1 and 3). However, the BG ionic extracts from 0.5 and 2.5 g/L BG inhibited SHEDs' proliferation at days 5 and 7. This effect could be caused by the more prolonged incubation of SHEDs with a high concentration of Si. High levels of Si had shown an inhibitory effect on cell growth and proliferation (Rismanchian et al., 2013; Zhou et al., 2013). Similarly, Gong et al. (2014) had reported an inhibitory effect of BG ionic extractions from 1 g/L BG on the proliferation of adult human dental pulp stem cells (hDPSCs). Our findings and reports from the literature suggest that the optimization of BG concentration is crucial to eliminate the cytotoxicity during BG-mediated pulp-dentin regeneration.

Dentin protects the dental pulp, and odontogenic differentiation of dental pulp stem cells is crucial for the maintenance and regeneration of dentin (Shah et al., 2020). Therefore, the biomaterials used for pulp-dentin revitalization should have odontogenic potential. Nanoscale BG had shown higher odontogenic potential compared to microscale BG (Gong et al., 2014; Wang et al., 2014). Ionic extractions from 1 g/L nano BG (10–100 nm) robustly enhance odontogenic differentiation of hDPSCs compared to ionic extractions from micro-scale BG (Gong et al., 2014). Similarly, 0.1 and 0.5 g/L of
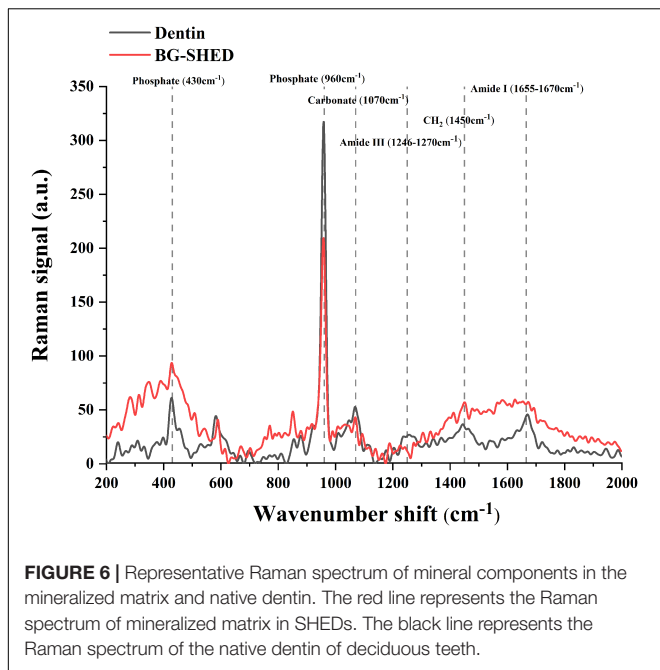
FIGURE 6 | Representative Raman spectrum of mineral components in the mineralized matrix and native dentin. The red line represents the Raman spectrum of mineralized matrix in SHEDs. The black line represents the Raman spectrum of the native dentin of deciduous teeth.

TABLE 2 | Normalized spectra intensity of mineral components.

Group	Phosphate peak (960 cm^{-1})	Mineral-to-matrix ratio	Carbonate-to-phosphate ratio
Native dentin	313.27 ± 5.05	10.12 ± 1.04	0.16 ± 0.01
Mineral matrix	207.47 ± 4.21	7.51 ± 2.72	0.20 ± 0.01

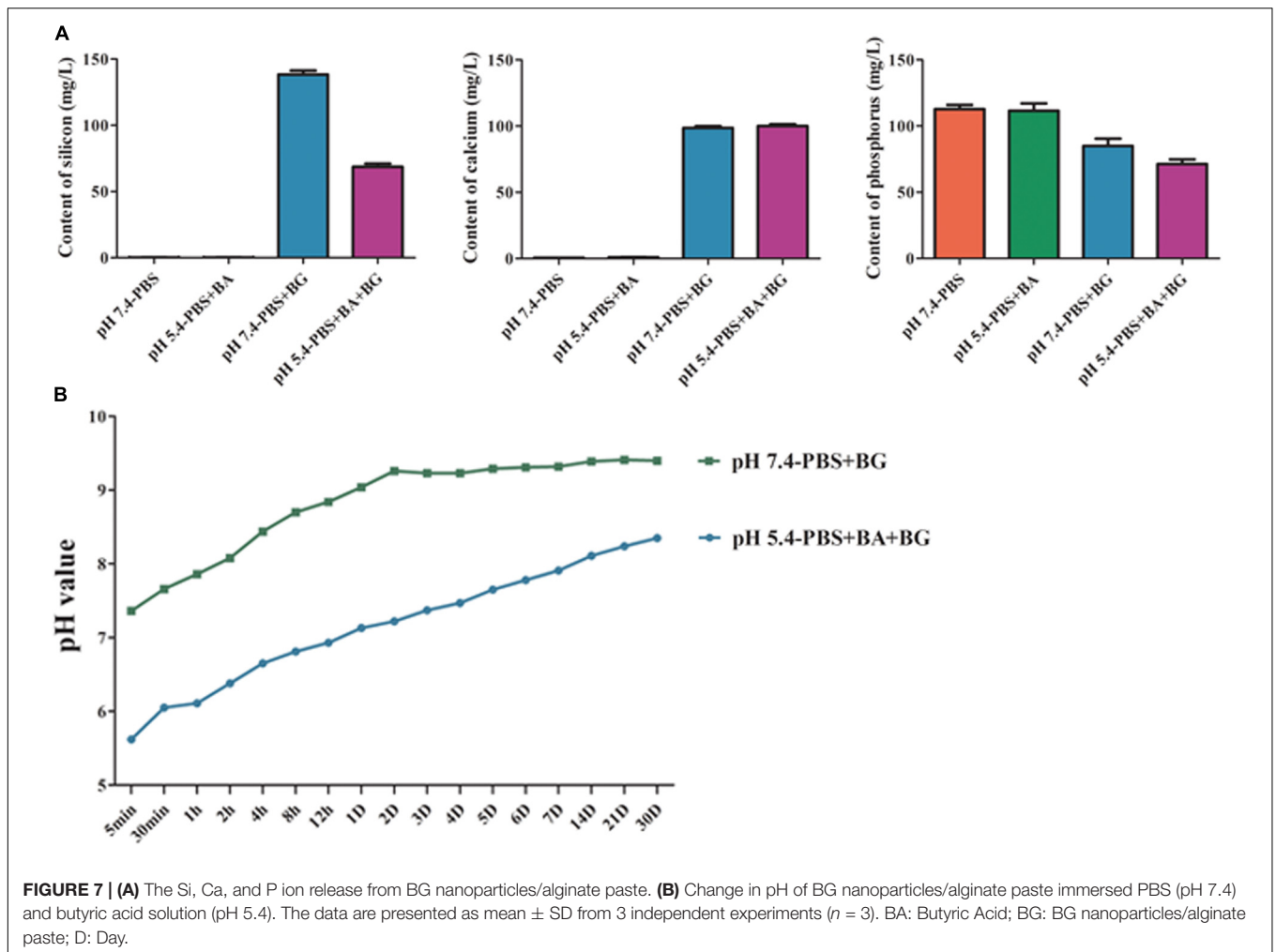*The data are presented as mean ± SD from 3 independent experiments (n = 3).*

BG nanoparticles (20 nm) enhance odontogenic differentiation of hDPSCs in dose-dependent manner (Wang et al., 2014). In this study, the ionic extraction from 0.5 g/L mesoporous BG showed the highest effect on the upregulation of odontogenic differentiation of SHEDs. BG ionic extraction from 0.5 g/L BG induced the higher expression of odontogenic markers and matrix mineralization in SHEDs culture compared to 0.1 and 2.5 g/L BG. This inhibitory effect of the BG ionic extraction from 2.5 g/L BG could be associated with the higher dose of Si induced cytotoxicity. Si concentration in BG ionic extract from 2.5 g/L BG was 1.7-fold higher than in BG ionic extract from 0.5 g/L BG. Our results rule out the dose-dependent anabolic effect of BG on odontogenesis, suggesting the importance of the optimal dose of BG in dentin-pulp regeneration. The difference between native dentin and mineralized matrix in SHEDs cultured with BG ionic extraction has not been investigated yet. We analyzed the mineral and organic contents in the BG-induced mineralized matrix in SHEDs culture. The most intense peak at 960 cm^{-1} was assigned to the dentin mineral phosphate, and the peak at 1070 cm^{-1} was assigned to the mineral carbonate (CO_3^{2-}). The peaks at 1246–1270, 1450, and 1655–1667 cm^{-1} were assigned to Amide III, CH_2, and Amide I, respectively, that are related to the organic composition in hard tissue (Wang et al., 2014). We confirmed for the first time that the chemical characteristics

of the mineralized matrix in SHEDs cultured with BG ionic extraction resembled native dentine. This result indicates the dentin regenerative potential of mesoporous BG nanoparticles.

Butyric acid and lactic acid are the main acidic byproducts of localized bacteria in the dental cavity (Hojo et al., 1994; Loesche, 1996), which could drop the pH below 5.5 in the decayed tooth cavity and affect pulp tissue homeostasis. Acidic pH not only affects the physicochemical biomaterial used but also impairs cell viability and activity (Hirose et al., 2016; Pushpa et al., 2018). Moreover, acidic pH also amplifies the inflammation in pulp tissue. Although mild inflammation is necessary for dentin-pulp tissue regeneration, the chronic and higher degree of inflammation will cause detrimental effects. Mesoporous BG nanoparticles not only have antimicrobial properties but also provides the nano-platform for antimicrobial strategies (Kargozar et al., 2018). In this study, we showed the butyric acid pH 5.4 neutralizing potential of mesoporous BG nanoparticles/alginate paste. BG/alginate paste was able to buffer pH of the butyric acid solution and PBS within pH 8.3 and 9.3, respectively. Neutral to pH 8.3 favors pH cell growth and activity. BG showed a markedly slower release of Si at a pH of 5.4 than at a pH of 7.4. Our findings suggest mesoporous BG nanoparticles as a potent biomaterial with pH buffering capacity, indicating its application in pulp-dentin regeneration in acidic pathophysiological environment.

Bacterial infection, inflammation, acidic pH, and immune reaction are the main factors affecting pulp-dentin regeneration (Schmalz and Smith, 2014; Jung et al., 2019; Shah et al., 2020). Synergistic activity of immune cells, mesenchymal stem cells, angiogenic, and neurogenic processes are involved in pulp-dentin restoration (Shah et al., 2020). BG had shown potential for immunomodulation, inflammation mitigation, odontogenesis, angiogenesis, neuron regeneration, and inhibition of microbial growth (Marquardt et al., 2014; Drago et al., 2015; Yu et al., 2016; Barbeck et al., 2017; Zhao et al., 2018; Farano et al., 2019; Gomez-Cerezo et al., 2019). We believe that the mesoporous BG nanoparticles designed in this study might have above-mentioned potentials, and could be used for various oral tissue regeneration, including pulp-dentin. Moreover, mesoporous BG nanoparticles could be the carrier of growth factors and antimicrobial agents needed during pulp-dentin regeneration.

In this study, we used the well-established sol-gel method to fabricate mesoporous BG nanoparticles. In comparison to BG nanoparticles, mesoporous BG nanoparticles have small size with higher specific surface area that enhances the bioactivity (Hu et al., 2014). Moreover, the mesoporous BG nanoparticles provide higher specific surface area to load desired drugs, proteins, and doping metal ions. The BG nanoparticles were well characterized, and the release of Si, Ca, and P ions from BG in a regular cell culture medium, acidic solution, and PBS were analyzed. Pulp/dentin regeneration of the hopeless tooth is still a challenge. Combination therapy of suitable biomaterial and stem cells could have the potential to regenerate the damaged pulp-dentin tissue. SHEDs have promising pulp-dentin regenerative potential and could be more easily harvested from deciduous teeth using a minimally invasive procedure compared to stem cells from permanent tooth pulp tissue. In

FIGURE 7 | (A) The Si, Ca, and P ion release from BG nanoparticles/alginate paste. **(B)** Change in pH of BG nanoparticles/alginate paste immersed PBS (pH 7.4) and butyric acid solution (pH 5.4). The data are presented as mean ± SD from 3 independent experiments ($n = 3$). BA: Butyric Acid; BG: BG nanoparticles/alginate paste; D: Day.

FIGURE 8 | Scheme of the ionic reaction of BG nanoparticles in a neutral or acidic environment.

this study, we used SHEDs as a source of stem cells to get insights on the possible use of mesoporous BG nanoparticles and SHEDs for pulp dentin regeneration. Dentin like mineralized matrix regenerative potential of BG nanoparticles in SHEDs culture was analyzed by comparing the chemical properties with native dentin using Raman spectroscopy. BG/alginate paste was fabricated, and the acidic pH neutralizing potential for one month was tested. A limitation of this study is that we did

not analyze the dentin regeneration of acidic pH neutralizing potential using *in vivo* set up. Future studies on pulp-dentin regeneration using mesoporous BG nanoparticles containing tooth sealing materials are strongly recommended. Moreover, the chemical, molecular, and cellular mechanism of BG-mediated pulp-dentin regeneration needs to be elucidated for the possible clinical applications.

CONCLUSION

In this study, spherical and mono-dispersed mesoporous BG nanoparticles were successfully fabricated and characterized. The BG nanoparticles showed odontogenic and dentin regenerative potential *in vitro*. Moreover, the BG nanoparticles/alginate paste neutralized the acidic pH 5.4 and buffered within pH 8.3 for a month. The concentration of Si ion release from BG in butyric acid solution (pH 5.4) was reduced by half compared to in PBS (pH 7.4). The findings of this study indicate the potential application of BG nanoparticles alone or in combination with SHEDs for pulp-dentin regeneration in pathophysiological acidic environment.

DATA AVAILABILITY STATEMENT

The raw data supporting the conclusions of this article will be made available by the authors, without undue reservation.

ETHICS STATEMENT

The studies involving human participants were reviewed and approved by The Research Ethics Committee of Guangzhou Medical University. Written informed consent to participate in this study was provided by the participants' legal guardian/next of kin.

AUTHOR CONTRIBUTIONS

WH, LG, JP, and SZ conceptualized and designed the study and reviewed the final manuscript. WH, JY, QF, YS, and HG acquired the data, analyzed the data, and wrote the manuscript. WH and JY performed *in vitro* experiments. CL and SZ prepared and characterized BG nanoparticles. All authors read and approved the submitted version.

FUNDING

REFERENCES

Akpinar, G., Kasap, M., Aksoy, A., Duruksu, G., Gacar, G., and Karaoz, E. (2014). Phenotypic and proteomic characteristics of human dental pulp derived mesenchymal stem cells from a natal, an exfoliated deciduous, and an impacted third molar tooth. *Stem Cells Int.* 2014:457059. doi: 10.1155/2014/457059

Azuma, M. (2006). Fundamental mechanisms of host immune responses to infection. *J. Periodont. Res.* 41, 361–373. doi: 10.1111/j.1600-0765.2006.00896.x

Barbeck, M., Serra, T., Booms, P., Stojanovic, S., Najman, S., Engel, E., et al. (2017). Analysis of the in vitro degradation and the in vivo tissue response to bi-layered 3D-printed scaffolds combining PLA and biphasic PLA/bioglass components - Guidance of the inflammatory response as basis for osteochondral regeneration. *Bioact. Mater.* 2, 208–223. doi: 10.1016/j.bioactmat.2017.06.001

Drago, L., De Vecchi, E., Bortolin, M., Toscano, M., Mattina, R., and Romano, C. L. (2015). Antimicrobial activity and resistance selection of different bioglass S53P4 formulations against multidrug resistant strains. *Future Microbiol.* 10, 1293–1299. doi: 10.2217/FMB.15.57

Elnaghy, A. M. (2014). Influence of acidic environment on properties of biodentine and white mineral trioxide aggregate: a comparative study. *J. Endod.* 40, 953–957. doi: 10.1016/j.joen.2013.11.007

Farano, V., Maurin, J. C., Attik, N., Jackson, P., Grosgogeat, B., and Gritsch, K. (2019). Sol-gel bioglasses in dental and periodontal regeneration: a systematic review. *J. Biomed. Mater. Res. B Appl. Biomater.* 107, 1210–1227. doi: 10.1002/jbm.b.34214

Gomez-Cerezo, N., Casarrubios, L., Saiz-Pardo, M., Ortega, L., de Pablo, D., Diaz-Guemes, I., et al. (2019). Mesoporous bioactive glass/varepsilon-polycaprolactone scaffolds promote bone regeneration in osteoporotic sheep. *Acta Biomater.* 90, 393–402. doi: 10.1016/j.actbio.2019.04.019

Gong, W., Huang, Z., Dong, Y., Gan, Y., Li, S., Gao, X., et al. (2014). Ionic extraction of a novel nano-sized bioactive glass enhances differentiation and mineralization of human dental pulp cells. *J. Endod.* 40, 83–88. doi: 10.1016/j.joen.2013.08.018

He, Z., Chen, L., Hu, X., Shimada, Y., Otsuki, M., Tagami, J., et al. (2017). Mechanical properties and molecular structure analysis of subsurface dentin after Er:YAG laser irradiation. *J. Mech. Behav. Biomed. Mater* 74, 274–282. doi: 10.1016/j.jmbbm.2017.05.036

Hench, L. L., and Jones, J. R. (2015). Bioactive glasses: frontiers and challenges. *Front. Bioeng. Biotechnol.* 3:194. doi: 10.3389/fbioe.2015.00194

Hench, L. L., and Polak, J. M. (2002). Third-generation biomedical materials. *Science* 295, 1014–1017. doi: 10.1126/science.1067404

Hirose, Y., Yamaguchi, M., Kawabata, S., Murakami, M., Nakashima, M., Gotoh, M., et al. (2016). Effects of extracellular pH on dental pulp cells in vitro. *J. Endod.* 42, 735–741. doi: 10.1016/j.joen.2016.01.019

Hojo, S., Komatsu, M., Okuda, R., Takahashi, N., and Yamada, T. (1994). Acid profiles and pH of carious dentin in active and arrested lesions. *J. Dent. Res.* 73, 1853–1857. doi: 10.1177/00220345940730121001

Hu, Q., Jiang, W. H., Li, Y. L., Chen, X. F., Liu, J. M., Chen, T., et al. (2018). The effects of morphology on physicochemical properties, bioactivity and biocompatibility of micro-/nano-bioactive glasses. *Adv. Powder Technol.* 29, 1812–1819. doi: 10.1016/j.apt.2018.04.017

Hu, Q., Li, Y. L., Miao, G. H., Zhao, N. R., and Chen, X. F. (2014). Size control and biological properties of monodispersed mesoporous bioactive glass submicron spheres. *RSC Adv.* 4, 22678–22687. doi: 10.1039/c4ra01276c

Jung, C., Kim, S., Sun, T., Cho, Y. B., and Song, M. (2019). Pulp-dentin regeneration: current approaches and challenges. *J. Tissue Eng.* 10:2041731418819263. doi: 10.1177/2041731418819263

Kargozar, S., Montazerian, M., Hamzehlou, S., Kim, H. W., and Baino, F. (2018). Mesoporous bioactive glasses: promising platforms for antibacterial strategies. *Acta Biomater.* 81, 1–19. doi: 10.1016/j.actbio.2018.09.052

Lee, S. J., Monsef, M., and Torabinejad, M. (1993). Sealing ability of a mineral trioxide aggregate for repair of lateral root perforations. *J. Endod.* 19, 541–544. doi: 10.1016/S0099-2399(06)81282-3

Lei, B., Chen, X. F., Han, X., and Zhou, J. A. (2012). Versatile fabrication of nanoscale sol-gel bioactive glass particles for efficient bone tissue regeneration. *J. Mater. Chem.* 22, 16906–16913. doi: 10.1039/c2jm31384g

Li, R., Clark, A. E., and Hench, L. L. (1991). An investigation of bioactive glass powders by sol-gel processing. *J. Appl. Biomater.* 2, 231–239. doi: 10.1002/jab.770020403

Li, Y. L., Liang, Q. M., Lin, C., Li, X., Chen, X. F., and Hu, Q. (2017). Facile synthesis and characterization of novel rapid-setting spherical sub-micron bioactive glasses cements and their biocompatibility in vitro. *Mater. Sci. Eng. C Mater. Biol. Appl.* 75, 646–652. doi: 10.1016/j.msec.2017.02.095

Lin, R., Deng, C., Li, X., Liu, Y., Zhang, M., Qin, C., et al. (2019). Copper-incorporated bioactive glass-ceramics inducing anti-inflammatory phenotype and regeneration of cartilage/bone interface. *Theranostics* 9, 6300–6313. doi: 10.7150/thno.36120

Loesche, W. J. (1996). "Microbiology of dental decay and periodontal disease," in *Medical Microbiology*, ed. S. Baron (Galveston, TX: University of Texas Medical Branch).

Lovelace, T. B., Mellonig, J. T., Meffert, R. M., Jones, A. A., Nummikoski, P. V., and Cochran, D. L. (1998). Clinical evaluation of bioactive glass in the treatment of periodontal osseous defects in humans. *J. Periodontol.* 69, 1027–1035. doi: 10.1902/jop.1998.69.9.1027

Marquardt, L. M., Day, D., Sakiyama-Elbert, S. E., and Harkins, A. B. (2014). Effects of borate-based bioactive glass on neuron viability and neurite extension. *J. Biomed. Mater. Res. A* 102, 2767–2775. doi: 10.1002/jbm.a.34944

Miura, M., Gronthos, S., Zhao, M., Lu, B., Fisher, L. W., Robey, P. G., et al. (2003). SHED: stem cells from human exfoliated deciduous teeth. *Proc. Natl. Acad. Sci. U.S.A.* 100, 5807–5812. doi: 10.1073/pnas.0937635100

Niederman, R., Buyle-Bodin, Y., Lu, B. Y., Robinson, P., and Naleway, C. (1997). Short-chain carboxylic acid concentration in human gingival crevicular fluid. *J. Dent. Res.* 76, 575–579. doi: 10.1177/00220345970760010801

Parirokh, M., and Torabinejad, M. (2010). Mineral trioxide aggregate: a comprehensive literature review–Part III: clinical applications, drawbacks, and mechanism of action. *J. Endod.* 36, 400–413. doi: 10.1016/j.joen.2009.09.009

Parirokh, M., Torabinejad, M., and Dummer, P. M. H. (2018). Mineral trioxide aggregate and other bioactive endodontic cements: an updated overview - part I: vital pulp therapy. *Int. Endod. J.* 51, 177–205. doi: 10.1111/iej.12841

Pushpa, S., Maheshwari, C., Maheshwari, S., Sridevi, N., Duggal, P., and Ahuja, P. (2018). Effect of pH on solubility of white mineral trioxide aggregate and biodentine: an in vitro study. *J. Dent. Res. Dent. Clin. Dent. Prospects* 12, 201–207. doi: 10.15171/joddd.2018.031

Rahaman, M. N., Day, D. E., Bal, B. S., Fu, Q., Jung, S. B., Bonewald, L. F., et al. (2011). Bioactive glass in tissue engineering. *Acta Biomater.* 7, 2355–2373. doi: 10.1016/j.actbio.2011.03.016

Rismanchian, M., Khodaeian, N., Bahramian, L., Fathi, M., and Sadeghi-Aliabadi, H. (2013). In-vitro comparison of cytotoxicity of two bioactive glasses in micropowder and nanopowder forms. *Iran J. Pharm. Res.* 12, 437–443.

Schepers, E., Declercq, M., Ducheyne, P., and Kempeneers, R. (1991). Bioactive glass particulate material as a filler for bone-lesions. *J. Oral Rehabil.* 18, 439–452. doi: 10.1111/j.1365-2842.1991.tb01689.x

Schmalz, G., and Smith, A. J. (2014). Pulp development, repair, and regeneration: challenges of the transition from traditional dentistry to biologically based therapies. *J. Endod.* 40(4 Suppl.), S2–S5. doi: 10.1016/j.joen.2014.01.018

Schwartz, A. G., Pasteris, J. D., Genin, G. M., Daulton, T. L., and Thomopoulos, S. (2012). Mineral distributions at the developing tendon enthesis. *PLoS One* 7:e48630. doi: 10.1371/journal.pone.0048630

Shah, D., Lynd, T., Ho, D., Chen, J., Vines, J., Jung, H. D., et al. (2020). Pulp-dentin tissue healing response: a discussion of current biomedical approaches. *J. Clin. Med.* 9:434. doi: 10.3390/jcm9020434

Skallevold, H. E., Rokaya, D., Khurshid, Z., and Zafar, M. S. (2019). Bioactive glass applications in dentistry. *Int. J. Mol. Sci.* 20:960. doi: 10.3390/ijms20235960

Vichery, C., and Nedelec, J. M. (2016). Bioactive glass nanoparticles: from synthesis to materials design for biomedical applications. *Materials* 9:288. doi: 10.3390/ma9040288

Wang, L., Pathak, J. L., Liang, D., Zhong, N., Guan, H., Wan, M., et al. (2020). Fabrication and characterization of strontium-hydroxyapatite/silk fibroin biocomposite nanospheres for bone-tissue engineering applications. *Int. J. Biol. Macromol.* 142, 366–375. doi: 10.1016/j.ijbiomac.2019.09.107

Wang, S., Gao, X., Gong, W., Zhang, Z., Chen, X., and Dong, Y. (2014). Odontogenic differentiation and dentin formation of dental pulp cells under nanobioactive glass induction. *Acta Biomater.* 10, 2792–2803. doi: 10.1016/j.actbio.2014.02.013

Yu, H., Peng, J., Xu, Y., Chang, J., and Li, H. (2016). Bioglass activated skin tissue engineering constructs for wound healing. *ACS Appl. Mater. Interf.* 8, 703–715. doi: 10.1021/acsami.5b09853

Yu, X., Wan, Q., Ye, X., Cheng, Y., Pathak, J. L., and Li, Z. (2019). Cellular hypoxia promotes osteogenic differentiation of mesenchymal stem cells and bone defect healing via STAT3 signaling. *Cell Mol. Biol. Lett.* 24:64. doi: 10.1186/s11658-019-0191-8

Zeng, D., Zhang, X., Wang, X., Huang, Q., Wen, J., Miao, X., et al. (2018). The osteoimmunomodulatory properties of MBG scaffold coated with amino functional groups. *Artif. Cells Nanomed. Biotechnol.* 46, 1425–1435. doi: 10.1080/21691401.2017.1369428

Zhao, F., Xie, W., Zhang, W., Fu, X., Gao, W., Lei, B., et al. (2018). 3D printing nanoscale bioactive glass scaffolds enhance osteoblast migration and extramembranous osteogenesis through stimulating immunomodulation. *Adv. Healthc. Mater.* 7:e1800361. doi: 10.1002/adhm.201800361

Zhou, H. M., Shen, Y., Wang, Z. J., Li, L., Zheng, Y. F., Hakkinen, L., et al. (2013). In vitro cytotoxicity evaluation of a novel root repair material. *J. Endod.* 39, 478–483. doi: 10.1016/j.joen.2012.11.026

Zhou, Y., Han, S., Xiao, L., Han, P., Wang, S., He, J., et al. (2018). Accelerated host angiogenesis and immune responses by ion release from mesoporous bioactive glass. *J. Mater. Chem. B* 6, 3274–3284. doi: 10.1039/c8tb00683k

Zhu, L., Luo, D., and Liu, Y. (2020). Effect of the nano/microscale structure of biomaterial scaffolds on bone regeneration. *Int. J. Oral Sci.* 12:6. doi: 10.1038/s41368-020-0073-y